

# Total absorption of unpolarized light by crossed gratings

E. Popov<sup>1</sup>, D. Maystre<sup>1</sup>, R.C.McPhedran<sup>1,2\*</sup>, M. Nevière<sup>3</sup>, M.C. Hutley<sup>4</sup> and G.H Derrick<sup>2</sup>

<sup>1</sup>Institut Fresnel, Aix-Marseille Université, CNRS, Domaine Universitaire de St Jérôme, case 161, 13397 Marseille Cedex 20, France

<sup>2</sup>CUDOS, School of Physics, University of Sydney, NSW 2006, Australia,

<sup>3</sup>Institut Universitaire de France, 103 boulevard Saint Michel, 75005 Paris, France,

<sup>4</sup>formerly of National Physical Laboratory, Teddington, Middlesex, U.K.

[ross@physics.usyd.edu.au](mailto:ross@physics.usyd.edu.au)

**Abstract:** We present both experimental and numerical data showing the absorption of unpolarized, normally incident light by a gold crossed grating having a shallow sinusoidal profile. We show furthermore that the total absorption of unpolarized light can be achieved for an angle of incidence of  $30^\circ$  with a crossed grating having its period adjusted appropriately from the normal incidence case to preserve the plasmonic resonance responsible for the enhanced absorptance. We contrast the process for achieving high absorptance in the principal plane of incidence aligned with the grooves of one of the gratings, with that for the principal plane at  $45^\circ$  to each grating.

© 2008 Optical Society of America

**OCIS codes:** (240.6680) Surface plasmons; (050.1950) Diffraction gratings; (050.5745) Resonance domain; (260.3910) Optics of metals.

---

## References and links

1. F.C. Garcia d'Abajo, "Colloquium: Light scattering by particle and hole arrays," *Rev. Mod. Phys.* **79**, 1267 (24 p) (2007).
2. R.W. Wood, "On a remarkable case of uneven distribution of light in a diffraction grating spectrum," *Phil. Mag.* **4**, 396-402 (1902).
3. J. Hagglund and F. Sellberg, "Reflection, absorption and emission of light by opaque optical gratings," *J. Opt. Soc. Am.* **56**, 1031-1040 (1966)
4. R.H. Ritchie, E.T. Arakawa, J.J. Cowan and R.N. Hamm, "Surface plasmon resonance effect in grating diffraction," *Phys. Rev. Lett.* **21**, 1530-1533 (1968).
5. R.C. McPhedran and M.D. Waterworth, "A theoretical demonstration of properties of grating anomalies (S polarization)," *Optica Acta* **19**, 877-892 (1972).
6. D. Maystre, "Sur la diffraction d'une onde plane par un réseau métallique de conductivité finie," *Opt. Commun.* **6**, 50-54 (1972).
7. M.C. Hutley and V.M. Bird, "Detailed experimental study of anomalies of a sinusoidal diffraction grating," *Optica Acta* **20**, 771-782 (1973).
8. R.C. McPhedran and D. Maystre, "A detailed theoretical study of the anomalies of a sinusoidal diffraction grating," *Optica Acta* **21**, 413-421 (1974).
9. D. Maystre and R. Petit, "Brewster incidence for metallic gratings," *Opt. Commun.* **17**, 196-200 (1976).
10. M.C. Hutley and D. Maystre, "The total absorption of light by a diffraction grating," *Opt. Commun.* **19**, 431-436 (1976).
11. G.H. Derrick, R.C. McPhedran, D. Maystre and M. Nevière, "Crossed gratings: a theory and its applications," *Appl. Phys.* **18**, 39-52 (1979).
12. R.C. McPhedran, G.H. Derrick and L.C. Botten, "Theory of Crossed Gratings," pp.227-276 in *Electromagnetic Theory of Gratings*, ed. R. Petit, Springer-Verlag (Heidelberg, 1980).
13. M. Nevière, D. Maystre, R. C. McPhedran, G.H. Derrick and M.C. Hutley, "On the total absorption of unpolarized monochromatic light," *Proceedings of the ICO-11 Conference, Madrid, Spain*, pp. 609-612 (1978).

14. R.C. McPhedran, G.H. Derrick, M. Nevière, and D. Maystre, "Metallic crossed gratings," *J. Opt.* **13**, 209-218 (1982).
  15. G.H. Derrick, R.C. McPhedran, and D.R. McKenzie, "Theoretical studies of textured amorphous silicon solar cells," *Appl. Opt.* **25**, 3690-3696 (1986).
  16. A. Avila-Garcia and U. Morales-Ortiz, "Thermally and air-plasma-oxidized titanium and stainless steel plates as solar selective absorbers," *Sol. En. Mat. and Sol. Cells* **90**, 2556-2568 (2006).
  17. S. Pillai, K.R. Catchpole, T. Trupke and M.A. Green, "Surface plasmon enhanced silicon solar cells," *J. Appl. Phys.* **101**, 093105 (8 pp.) (2007).
  18. F. Ghmari, T. Ghbara, M. Laroche, R. Carminati and J.J. Greffet, "The influence of microroughness on emissivity," *J. Appl. Phys.* **96**, 2656-2664 (2004).
  19. S. Zou and G. C. Schatz, "Narrow plasmonic/photonic extinction and scattering line shapes for one and two dimensional silver nanoparticle arrays," *J. Chem. Phys.* **121**, 12606-12612 (2004).
  20. J. Dintinger, S. Klein and T.W. Ebbesen, "Molecule-surface plasmon interactions in hole arrays: Enhanced absorption, refractive index changes, and all-optical switching," *Adv. Mat.* **18**, 1267-1270 (2006).
  21. J. Chandezon, D. Maystre and G. Raoult, "A new theoretical method for diffraction gratings and its numerical application," *J. Opt.-Nouv. Rev. d'Opt.* **11** 235-241 (1980).
  22. Lifeng Li and J. Chandezon, "Improvement of the coordinate transformation method for surface-relief gratings with sharp edges," *J. Opt. Soc. Am. A* **13**, 2247-2255 (1996).
  23. L. Mashev and E. Popov, "Conical diffraction mounting generalization of a rigorous differential method," *J. Opt.-Nouv. Rev d'Opt.* **17**, 175-180 (1986).
  24. G. Granet, "Analysis of diffraction by surface-relief crossed gratings with use of the Chandezon method: application to multilayer crossed gratings," *J. Opt. Soc. Am. A* **15**, 1121-1131 (1998).
- 

## 1. Introduction

A recent review article [1] has highlighted the surprising phenomena such as enhanced transmission which can occur due to the strong interactions possible between electromagnetic waves and periodic structures incorporating metals. We will discuss here another such surprising phenomenon: the enhanced and even total absorption which can occur when an incident light beam strikes a highly reflecting metal surface which has had a quite shallow grating superimposed on it. This phenomenon arises due to resonances which can occur due to the interaction between the light beam and the periodic structure, mediated by currents which can flow along the metal surface. Such resonances were highlighted as early as 1902 by R.W. Wood [2] in his classic paper on diffraction anomalies.

The association between diffraction anomalies and enhanced absorption by metallic gratings was studied in the 1960's by Hagglund and Sellberg[3], while soon afterwards Ritchie et al [4] established the importance of surface plasmon phenomena on diffraction gratings in the anomalous region. Theoretical studies were commencing around the same period using integral equation and differential methods, and an early study [5] of diffraction anomalies showed that good agreement between experiment and theory could be achieved with data from metallic gratings in the mid-infrared and longer wavelength regions, but that significant differences existed between calculations and measurements in the visible region. This difficulty was removed when the first integral equation method for gratings capable of taking into account the actual optical properties of metals was established by D. Maystre [6]. The theory was soon applied to the first laser measurements of diffraction grating efficiencies in the region of anomalous absorption [7], with very good quantitative agreement [8].

The first prediction concerning the possibility of achieving total absorption of polarized light by a metallic diffraction grating was made by Maystre and Petit [9], using a phenomenological model based on the poles and zeros of the grating diffraction efficiency, and in particular their locations in the plane of complex angle of incidence. The prediction was soon followed by an experimental verification [10].

The topic we address in this paper is that of the possibility of the total absorption of *unpolarized* light by a metallic grating. The strong polarization dependence of the properties of singly-periodic metallic diffraction gratings makes this difficult or impossible to achieve, so

a natural idea is to achieve polarization independence using a square-symmetric, doubly periodic diffraction grating, also called a bigrating or crossed grating. The implementation of this idea became possible once the first diffraction theories of periodic, doubly-modulated metallic surfaces were elaborated [11, 12], and its numerical prediction was once again followed by an experimental verification [13]. Since this last article is neither generally available nor electronically locatable, we make available its essential elements as part of this paper.

The initial applications proposed for doubly-periodic metallic diffraction gratings concerned use of their enhanced absorption for solar energy applications, either using photothermal [14] or photovoltaic [15] effects. Interest in both these topics continues [16, 17], while other applications have emerged, such as structured surfaces for the control of thermal emission [18], plasmonic sensing [19] and all-optical switching [20]. These have been spurred by the advances in available technologies for the fabrication and control of surface morphologies on the sub-micron scale, while the widespread interest in the physics of photonic crystals has made the use of doubly-periodic structures for control of light quite self evident.

The next section contains the details and results of an experimental demonstration of the near-total absorption of unpolarized light by a shallow crossed grating in gold with a symmetric sinusoidal profile, together with corresponding numerical results obtained by the rigorous surface transformation method [21, 22, 23] as generalized to doubly-periodic surfaces by Granet [24]. In the following section, we present numerical results showing the possibility of achieving total absorption of unpolarized light with a *non-normal* incident wave. This represents a considerable extension of the previous demonstrated capability for normally-incident light, and may open up new applications in terms of control of thermal emission and efficient launching of surface plasmons. We end by showing that it is possible to achieve lower reflectance in the case of incidence in a plane parallel to the grooves of one of the gratings, than for the case in which the incidence is in the plane at 45° to the grooves of either grating.

## 2. Total absorption by a metallic crossed grating at normal incidence

In Fig. 1 (a) we show the reflectance as a function of wavelength for gold classical gratings used with normally incident light, for both principal polarizations TE and TM, respectively with the incident electric field and the incident magnetic field along the grooves of the grating. Note that for wavelengths below the period (0.62 μm) of the grating, the orders -1 and 1 become propagating, although the reflected energy in Fig. 1 (a) is just that carried in the zeroth order. Note the diffraction anomaly (Rayleigh wavelength) apparent for TM polarization when the wavelength equals the period, with the TE data showing very a very weak reaction to the creation of the orders ±1, due to the shallow grating depth. Of course, the main feature of interest in Fig. 1 (a) is the plasmon resonance near 0.65 μm, which leads to a complete suppression of reflectance there. Fig. 1(a) has been calculated with the Chandezon method for classical gratings [21]-[23]. In Fig. 1(b) we compare this with the reflectance for a crossed grating composed of two gratings identical to that of Fig. 1(a), but with their periods at right angles, calculated with the transformation method of Granet [24]. The profile is given by

$$y = f(x, z) = h_x \sin\left(\frac{2\pi}{d_x}x\right) + h_z \sin\left(\frac{2\pi}{d_z}z\right) = h_x \sin(K_x x) + h_z \sin(K_z z). \quad (1)$$

Note that the grating has square symmetry, so that for normally incident light the reflectance is independent of polarization (for a discussion of symmetry properties of crossed gratings, see for example [15]). Note also the very interesting result that the crossed grating reflectance falls to zero at exactly the same point as that in Fig. 1 (a) or its constituent classical grating, and that the TM points from Fig. 1(a) for the classical grating coincide to graphical accuracy with the crossed grating results in the region of resonant absorption. This type of result has

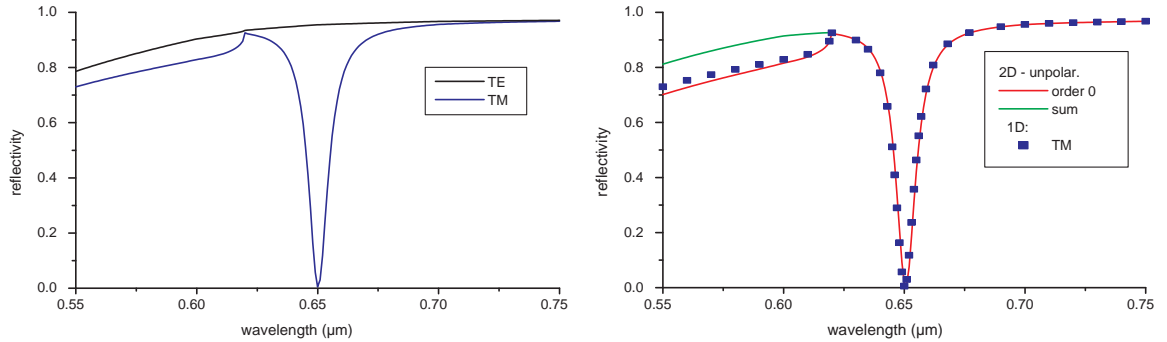


Fig. 1. (a) Spectral dependence of the 0-th order reflectivity of a shallow sinusoidal grating in normal incidence. Period  $d = 0.62\mu\text{m}$  and groove depth  $h = 0.032\mu\text{m}$ , polarization TE, parallel (black) or TM, perpendicular (blue) to the groove direction. (b) Same as in (a) but for a 2D crossed grating representing the sum of two mutually perpendicular gratings identical to the one in (a).  $d_x = d_z = 0.62\mu\text{m}$ ,  $h_x = h_z = 0.032\mu\text{m}$ , normal incidence. Order 0 in reflection - red, sum of orders 0 and -1 - in green, TM efficiency from Fig.1a - blue squares.

been interpreted in terms of an equivalence rule, linking efficiencies of crossed gratings with those of their constituent classical gratings (see [12]), but the accuracy of the correspondence between the classical grating and the crossed grating reflectances is very striking.

In order to test this prediction, a crossed grating was constructed by recording interference patterns of plane waves in photoresist, with the angle between the beams being adjusted to give a common period along the two axes of 600 nm. The depth of the grating was estimated using a chisel profilometer, whose stylus was too wide to penetrate the full depths of the modulations, so the depths of the grooves of the two orthogonal component gratings were measured independently, and their sum was taken to be the total depth (80 nm).

The reflectance as a function of wavelength for the crossed grating was measured using a combination of white light and laser sources. A collimated beam of white light was divided into two with a cube beam splitter. The beams were then reflected back down their own paths and into the slit of a monochromator either by the grating or by an aluminium reference mirror. The flux from each was detected with a photomultiplier and was selected by inserting a shutter as appropriate. In this way the ratio of the flux from the mirror and from the grating was measured as a function of wavelength throughout the visible region. This gave an approximate reflectance curve, which was normalised by direct measurements of the reflectance at a few discrete wavelengths from a krypton laser, using a power meter.

The comparison between theory and experiment in Fig. 2 shows very good agreement. There is a very slight wavelength shift between the two curves, which we can attribute to a slightly different period between the experimental grating and that used in the calculations. (Note that the wavelength difference between the reflectance minima in calculations and measurements is just the same as that between the positions of the diffraction anomalies, which occur here when the wavelength equals the period.) Both theory and experiment give a reflectance minimum near 3.5%, non-zero because of the grating depth slightly above the optimal value.

### 3. Total absorption by a metallic crossed grating at non-normal incidence

We now consider the interaction between a crossed grating whose profile is a sum of sinusoids as in equation (1) with an incident plane wave, whose incident wavevector has magnitude  $k_i =$

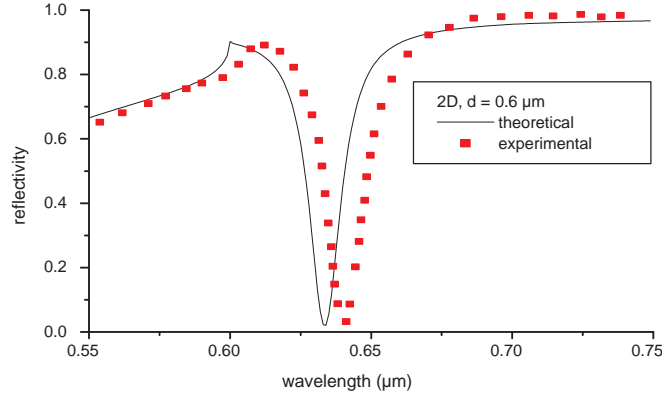


Fig. 2. Comparison between the theoretical and experimental reflectivity in normal incidence of a grating similar to Fig.1, but having period  $d_x = d_z = 0.6\mu\text{m}$  and total groove depth  $h = 0.08\mu\text{m}$  ( $h_x = h_z = 0.04\mu\text{m}$ ). Theoretical results - black curve, experimental data - red squares.

$2\pi/\lambda$  and is characterized in direction by the declination angle  $\theta_i$  and the azimuthal angle  $\phi_i$ :

$$\vec{k}_i = (\sin \theta_i \cos \phi_i, \cos \theta_i, \sin \theta_i \sin \phi_i) = (\alpha_i, -\beta_i, \gamma_i). \quad (2)$$

The crossed grating is covered with a highly conducting metal such as gold, which can support the propagation of surface plasmons. We think of the incident wave firstly as interacting with the two classical gratings which are added together in equation (1), as shown in Fig. 3.

The interaction shown in Fig. 3(a) is between the incident plane wave and the grating in  $x$  and occurs in classical diffraction. The equation linking the  $x$  components of the incident wavevector and the real part of the complex vector  $\vec{k}_{p,1}$  describing the first plasmon is

$$k_0 \alpha_i - K_x \simeq \Re(\vec{k}_{p,1})_x, \quad (3)$$

noting that the plasmon is associated with the order -1 of grating diffraction. The same incident wave is shown in Fig. 3(b) interacting in conical diffraction with the grating in  $z$ , and for this case two plasmons are created, travelling at the same angle to the  $x$  axis, and with equations expressing conservation of momentum in the  $x-z$  plane written in component form as

$$\Re(\vec{k}_{p,2}) = k_0(\alpha_i, \gamma_i), \quad \Re(\vec{k}_{p,3}) = k_0(\alpha_i, -\gamma_i). \quad (4)$$

Our goal is to exploit these individual resonances to find classical gratings which absorb completely the incident beam, and then to see whether an appropriate superposition of these two optimized classical gratings can provide a crossed grating capable of totally absorbing the incident beam, irrespective of its state of polarization. We first make one choice to facilitate this, by arranging the incident beam to lie in one of the principal planes ( $Oxy$ ) of the crossed grating ( $\phi_i = 0^\circ$  or equivalently  $\phi_i = 90^\circ$ ). We comment later on the other possible choice, with  $\phi_i = 45^\circ$ . We choose the other angle characterizing the incident wave to be  $\theta_i = 30^\circ$ .

Figure 4 shows the results of this process, with the numerical values for reflectance being provided by the Chandezon transformation method for classical gratings with in-plane mount, classical gratings in conical diffraction, and crossed gratings [21]-[24]. To obtain the first optimized classical grating of Fig. 4(a) we work with the geometry of Fig. 3(a), and we first adjust the period  $d_x$  to ensure the plasmon resonance condition (3) is satisfied at  $\lambda = 0.65\mu\text{m}$ , and then

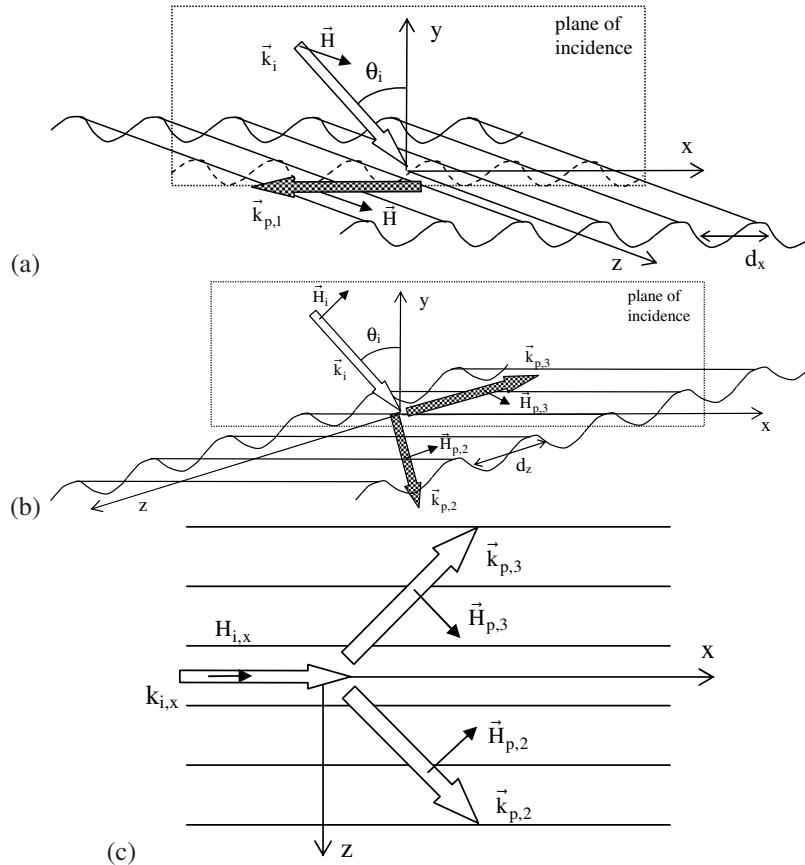


Fig. 3. Schematic representation of the incident wave vector and the plasmons excited by the surface corrugation for two gratings having modulation along two perpendicular axes, with the plane of incidence perpendicular to the  $z$  axis: (a) periodicity along  $x$ , i.e., classical diffraction with  $\vec{k}_i$  perpendicular to the grooves, exciting a single surface plasmon wave in TM incident polarization; (b) periodicity along  $z$ , conical diffraction exciting two surface plasmon waves in TE incident polarization; (c) view from above of (b).

the depth  $h_x$  and (with fine adjustment  $d_x$ ) to ensure total absorption at the target wavelength. To optimize the second grating of Fig. 4(a), that working in conical diffraction as in Fig. 3(b), it is first necessary to adjust the period  $d_z$  to achieve a plasmon resonance at the target wavelength ( $0.65 \mu\text{m}$ ) in accord with equation (4), and then the depth  $h_z$  and (with fine adjustment  $d_z$ ) to achieve the total absorptance curve shown.

When these two optimized gratings are combined to form a crossed grating, the reflectance curves for TE and TM polarizations are shown in Fig. 4(b). Note that the interaction of the two gratings causes the TM curve to lift up slightly, giving a minimum reflectance value of around 4%, while it causes the TE curve to shift slightly in frequency. The final step in the process to achieve the near total absorption in unpolarized light shown in Fig. 4(c) is a numerical readjustment varying the four parameters ( $d_x, h_x, d_z, h_z$ ) in a region close to the values of Fig. 4(b).

We note from Fig. 4(a-c) that the addition of constituent gratings alters the optimum properties of the structure for the principal polarizations. To clarify this effect further, we show in

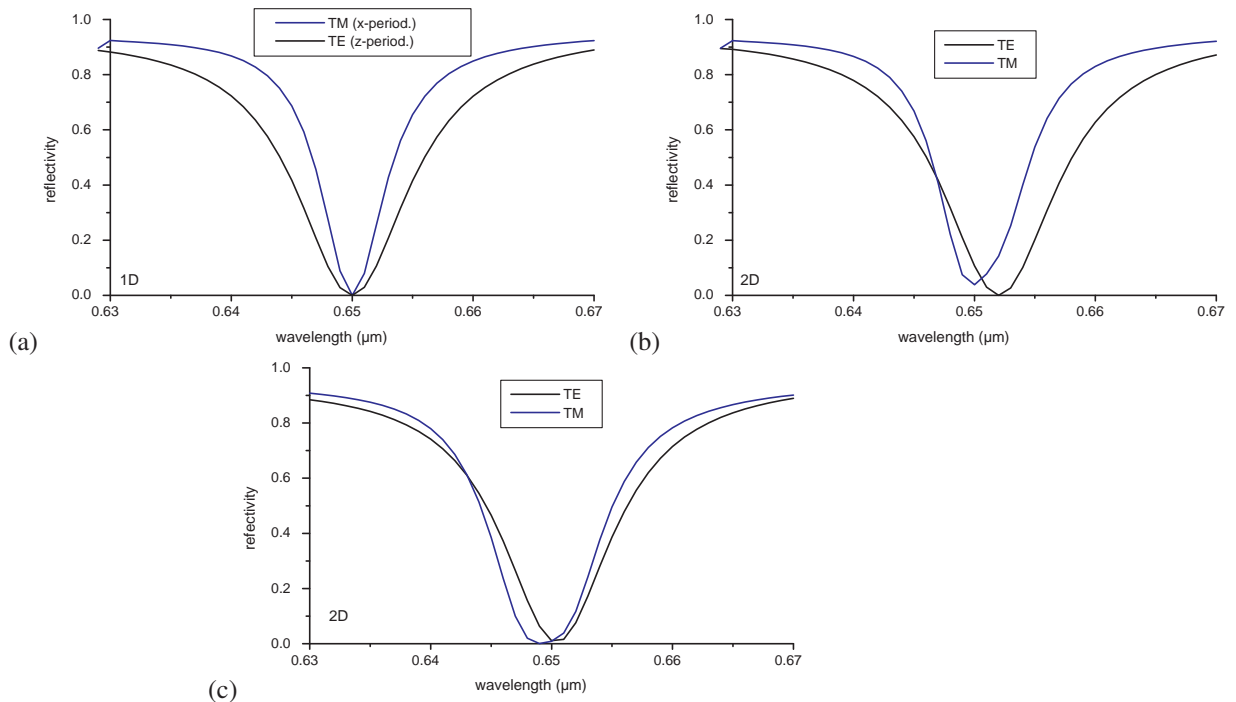


Fig. 4. Spectral dependence of the reflectivity at  $\theta_i = 30^\circ$ ,  $\gamma_i = 0$  and  $\lambda = 0.65 \mu\text{m}$  of: (a) two 1D sinusoidal gratings, as shown in Figs.3a and b, respectively, having parameters optimized for totally absorbing incident light. Grating 1 (blue)-  $d_x = 0.4199\mu\text{m}$ ,  $h_x = 0.0281\mu\text{m}$ , TM polarization with respect to the plane of incidence. Grating 2 (black)-  $d_z = 0.705\mu\text{m}$ ,  $h_z = 0.039\mu\text{m}$ , TE incident polarization. (b) 2D grating with a profile represented as a sum of the two gratings in (a). (c) 2D gratings with profile parameters optimized so as to totally absorb incident nonpolarized light:  $d_x = 0.419\mu\text{m}$ ,  $d_z = 0.701\mu\text{m}$ ,  $h_x = h_z = 0.037\mu\text{m}$ . Results for two mutually orthogonal incident polarizations.

Fig. 5 the effect, at fixed wavelength, on the curve of reflected energy versus groove depth  $h_x$  of adding the second constituent grating with fixed depth  $h_z = 0.04\mu\text{m}$ . It will be noted that this addition not only moves the position of the minimum reflectance point, but also alters the shape of the curve in the region near the minimum. We confirm with this result the deduction that the second grating interacts with the first, in such a way that the position of optimum absorption is changed by their interaction, by contrast with that which was obtained for normal incidence. The optimization of each separately is a useful first step, but the best performance requires a final optimization in which all the crossed grating parameters are jointly varied.

#### 4. Search for a totally absorbing crossed grating in the plane at $\theta_i = 45^\circ$

For the case of incidence in the plane at  $45^\circ$  to both constituent gratings, we have the situation where the two plasmon modes shown schematically in Fig. 6 propagate symmetrically with respect to both. This geometric symmetry means that the optimization of the crossed grating to maximize its absorptance at a target wavelength proceeds with the choices  $d_x = d_z$ ,  $h_x = h_z$  enforced. The numerical optimization of the two parameters period and depth then results in different parameters for the two fundamental polarizations TE and TM, as shown in Fig. 7: the periods do not differ significantly, but the depths differ by around 20%, resulting in a minimal



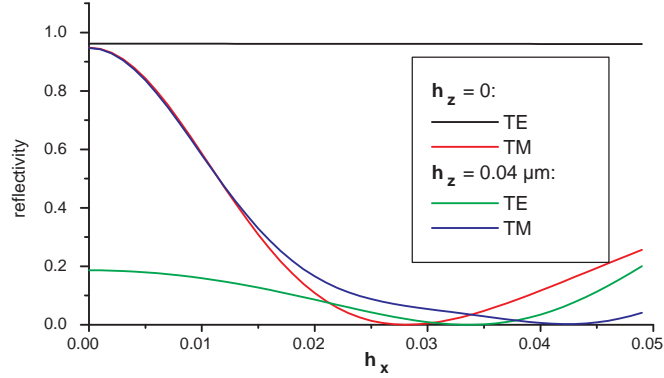


Fig. 5. The influence of the second groove depth ( $h_z$ ) of the 2D grating described in Fig.4 (b), on its reflectivity as a function of the first groove depth ( $h_x$ ) when  $\lambda = 0.65\mu\text{m}$ .

reflectance in unpolarized light (not shown in Fig. 7, but calculated) also close to 20%.

This result is disappointing compared with that of Section 3, and may be viewed from two different standpoints. Firstly, to achieve total absorptance in unpolarized light for  $\theta_i = 0, 90^\circ$ , we had at our disposition four variables:  $d_x, h_x, d_z, h_z$ , evidently sufficient to achieve zero reflectance in both fundamental polarizations at the same wavelength. The ability to vary only two quantities for  $\theta_i = 45^\circ$  is insufficient to achieve zero reflectance for two orthogonal polarizations at the same wavelength.

The second way of making this comparison is to note the differences between Fig. 3 and Fig. 6 in the way the plasmons interact with the constituent gratings. In the first case, the constituent gratings give plasmons propagating in different directions, and thus it is clear that they can be controlled more or less separately using different grating parameters. In the second case, the plasmons propagate in the same direction but have different field symmetries, which may indicate the need for more complicated profiles than that of equation (1) if fields of differing symmetries are to be controlled largely independently.

For example, in TM incident polarization, as seen in Fig. 6(a), the two plasmons form a magnetic field combination that is symmetric with respect to the plane of incidence, whereas the TE case (Fig. 6(b)) requires an antisymmetric magnetic field distribution. As happens in many instances in physics, symmetric and antisymmetric solutions have different resonant wavelengths, as observed in Fig. 7.

## 5. Enhanced absorption as a function of angular direction

Numerical results presented above are obtained using plane incident waves. In practice, incident beams are always limited in size and thus it is interesting to study the angular dependence of the reflectivity. Figs.8(a - c) present the reflectivity as a function of  $\alpha_i$  and  $\gamma_i$  for both TE (a) and TM (b) polarization, together with the unpolarized case (c), which is the average of the first two cases. The effect of almost total absorption persists along several lines which can be easily determined from the geometrical condition of excitation of different plasmon surface waves, as determined by eqs.(3) and (4). In TE polarization, these conditions imply that

$$\alpha_i^2 + (\gamma_i \mp K_z)^2 \simeq \Re(k_p^2), \quad (5)$$

which represents two circles with radius  $\Re(k_p)$  centred at  $(0, 0, \pm K_z)$ . Two arcs of these circles can be observed as minima of the reflectivity in Fig.8(a). In TM polarization, the excitation of



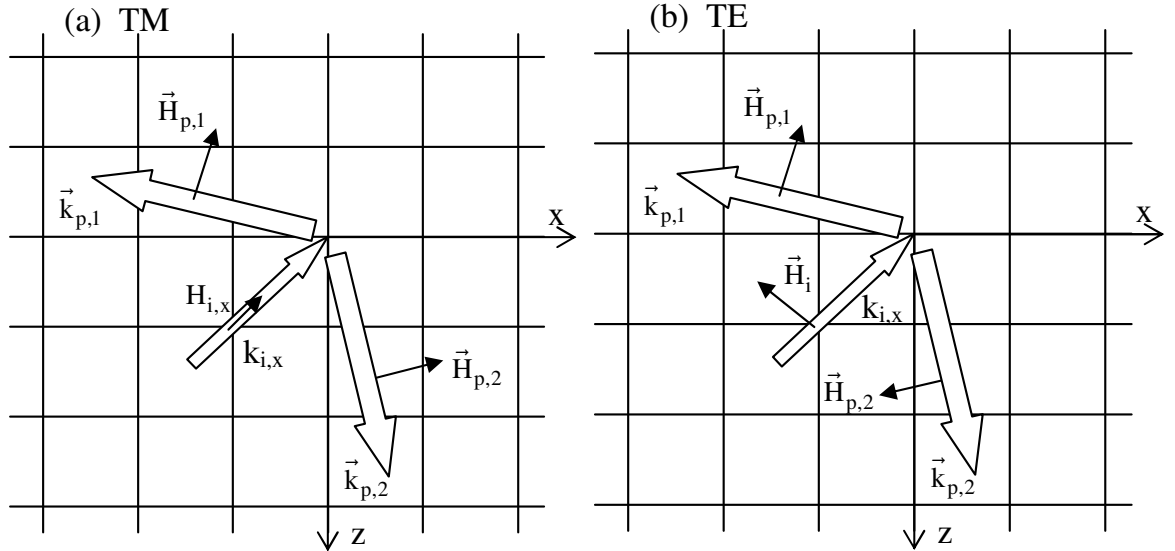


Fig. 6. Schematic representation of surface plasmon excitation by a crossed grating with the plane of incidence at  $45^\circ$  with respect to the groove directions. (a) Symmetric magnetic field mode, (b) antisymmetric mode.

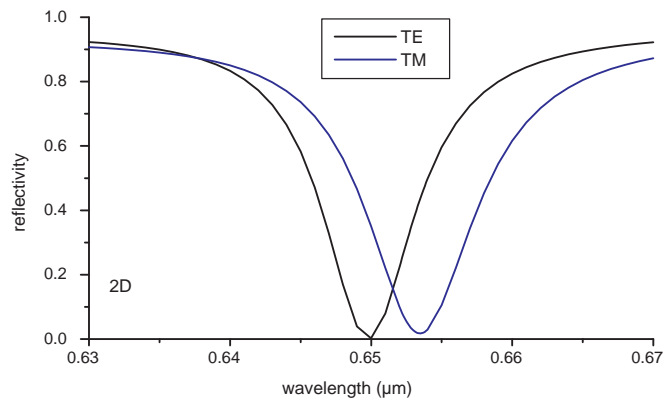


Fig. 7. Spectral dependence of efficiencies in two fundamental incident polarizations with plane of incidence at  $45^\circ$  to the  $x$ - and  $z$ -axes. Black, TE,  $d_x = d_z = 0.485\mu\text{m}$ ,  $h_x = h_z = 0.038\mu\text{m}$ , blue, TM,  $d_x = d_z = 0.483\mu\text{m}$ ,  $h_x = h_z = 0.032\mu\text{m}$ .

the plasmon surface wave follows the condition:

$$(\alpha_i \mp K_x)^2 + \gamma_i^2 \simeq \Re(k_p^2), \quad (6)$$

which represents circles with radius  $\Re(k_p)$  centred at  $(\pm K_x, 0, 0)$ . An arc of one of these circles is evident and can be traced in Fig.8(b). The combined effect of the TE and TM curves is shown in Fig. 8(c), for unpolarized light. This enables [18] the visualization of the emission pattern for radiation at  $\lambda = 0.65\mu\text{m}$  by the crossed grating: the maximum power would be radiated in unpolarized light around the direction given by  $\alpha_i = 0.5$ ,  $\gamma_i = 0$ , while polarized light would be emitted along the three arcs of circles.

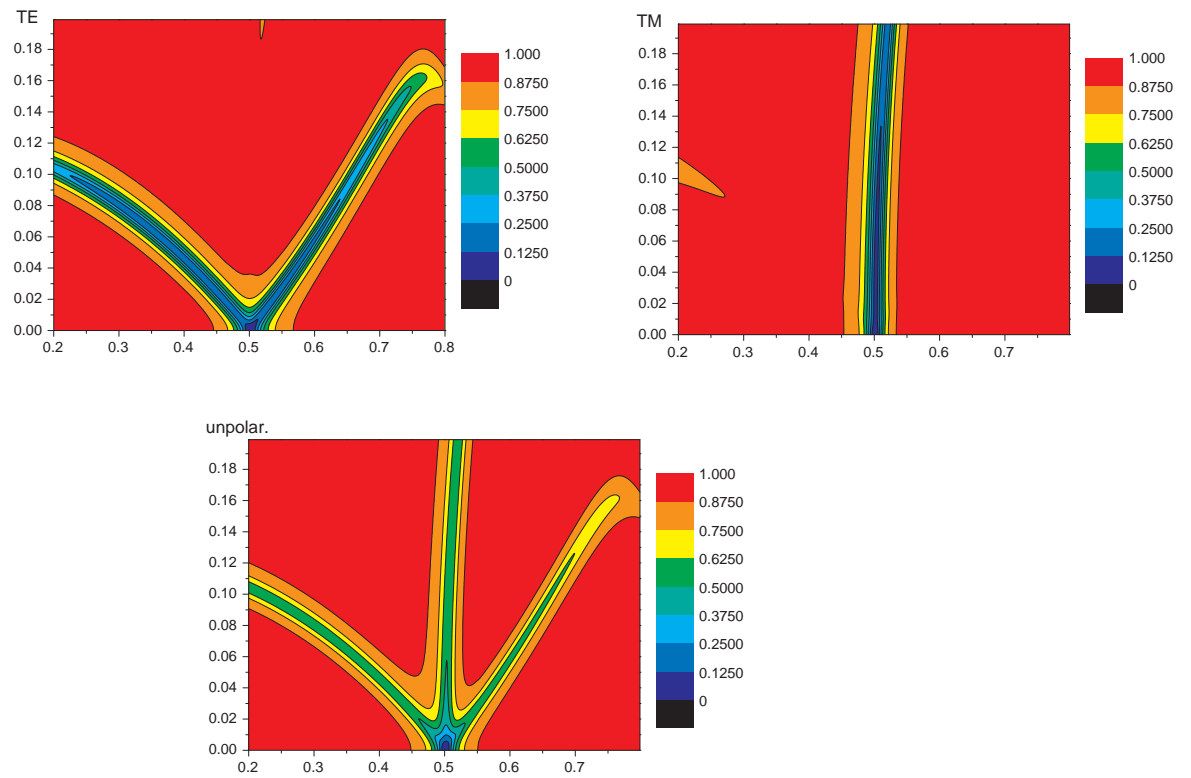


Fig. 8. Reflectivity as a function of  $\alpha_i$  (horizontal axis) and  $\gamma_i$  (vertical axis) for TE polarization (a), TM polarization (b) and unpolarized light (c), for the crossed grating of Fig. 4(c).

#### Acknowledgements:

Ross McPhedran acknowledges support from the Australian Research Council's Discovery Projects Scheme. His work on this project was also supported by the C.N.R.S., France.